Supporting Information

Site-dependent catalytic activity of graphene oxides towards oxidative dehydrogenation of propane

Shaobin Tang[a] and Zexing Cao[b,]*

[a]Key Laboratory of Organo-Pharmaceutical Chemistry of Jiangxi Province, Gannan Normal University, Ganzhou 341000, China
[b]State Key Laboratory of Physical Chemistry of Solid Surfaces and Fujian Provincial Key Laboratory of Theoretical and Computational Chemistry, College of Chemistry and Chemical Engineering, Xiamen University, Xiamen 361005, China

*Corresponding author e-mail: zxcao@xmu.edu.cn

1. Optimized structures and spin densities of formed C_3H_7 on GOs.

The spin densities calculations (Figure S1) show that the net magnetic moments of C_3H_7 on various GO structures are mainly contributed by the carbon atom in CH_2, suggesting that formation of propyl radical after the first H atom abstraction. The formed C_3H_7 species is physisorbed on GO surface without any covalent bond interaction.

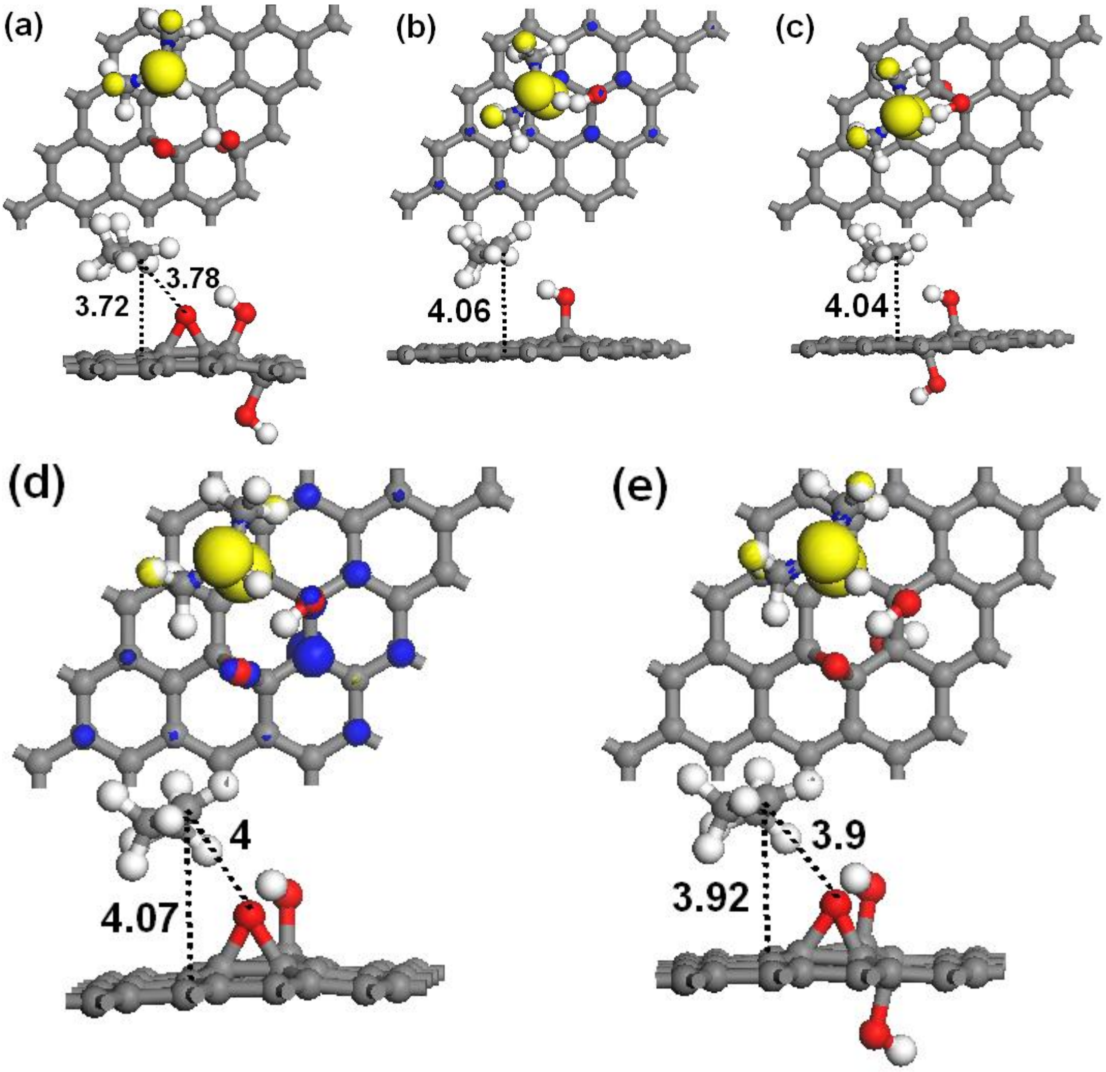

Figure S1. Optimized structures (top and side view) and spin densities (top view) of formed C_3H_7 (distance in Å) on (a) GO2, (b) GO1', (c) GO2', (d) GO1'', and (e) GO2''. The isosurface is 0.03 e/Å^3 with blue for spin up and yellow for spin down.

2. Optimized structures and energy profiles for the conversion from propane to C_3H_7 on GO with the larger graphene supercells.

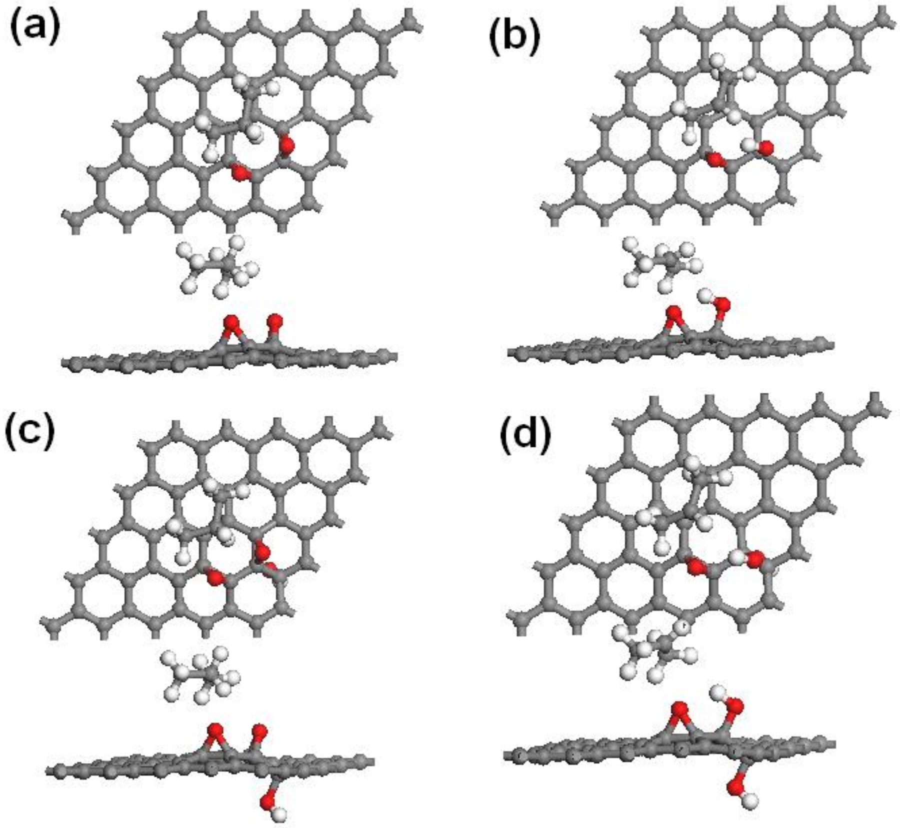

Figure S2. Top and side view of optimized structures for the conversion from propane to C_3H_7 on GO with 5×5 supercells. (a) and (c) Adsorption of propane, (b) and (d) formation of C_3H_7.

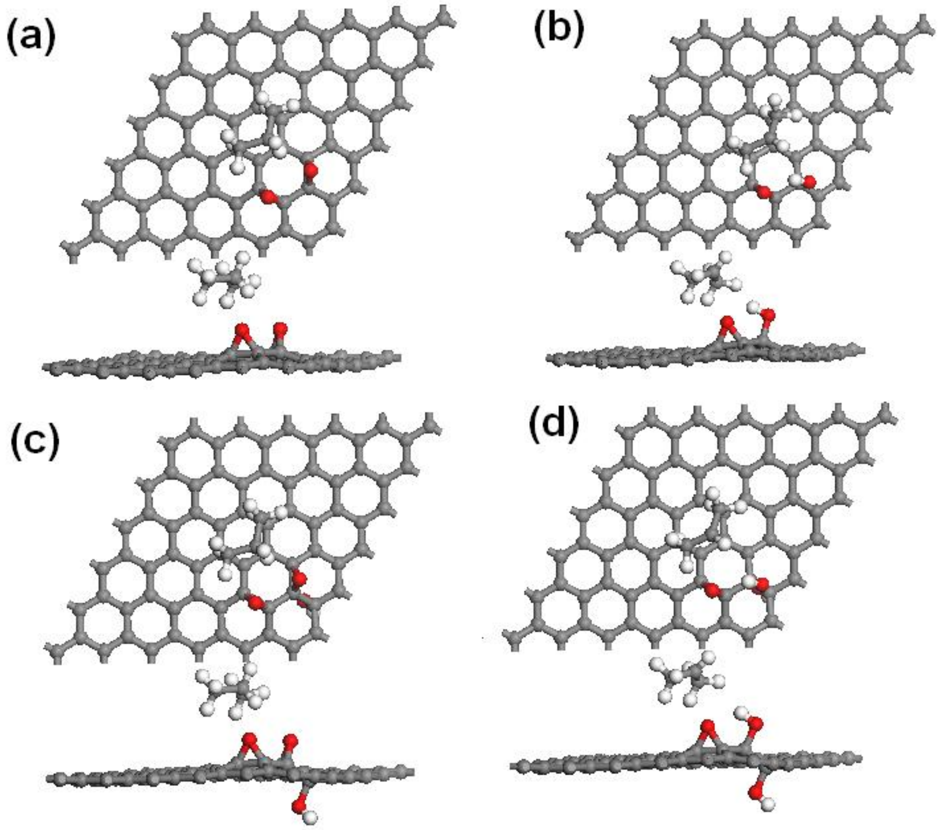

Figure S3. Top and side view of optimized structures for the conversion from propane to C_3H_7 on GO with 6×6 supercells. (a) and (c) Adsorption of propane, (b) and (d) formation of C_3H_7.

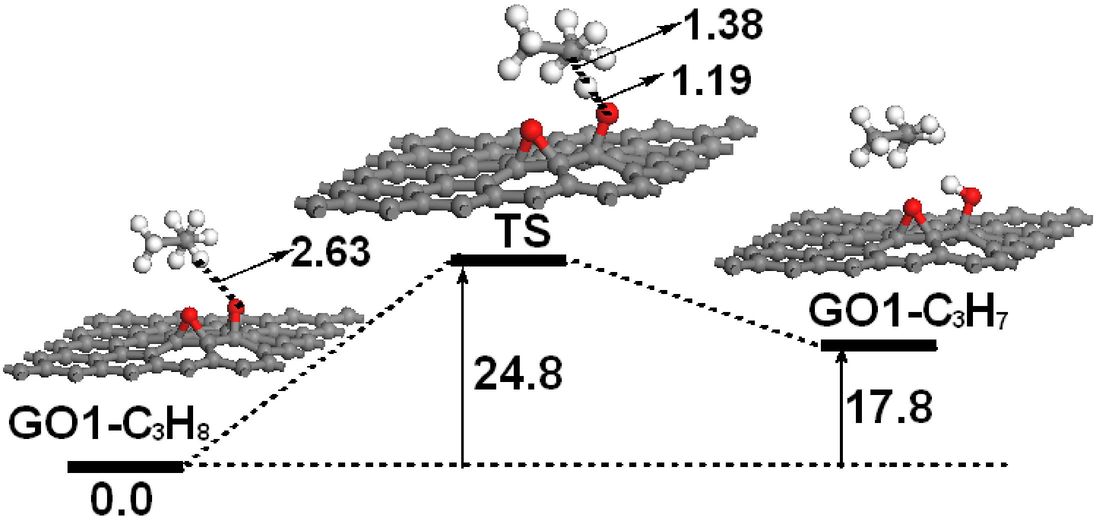

Figure S4. Energy profiles for the first H abstraction from CH_2 of propane on GO1 with 5×5 supercells. All energies (in kcal/mol) are relative to propane adsorbed on GO1, and the optimized configurations (distance in Å) of initial, transition, and final states are shown.

3. Optimized structures, spin densities, relative energy profiles for conversion from propane to C_3H_7 on GO2 with the adsorbed OH group at d and e site.

The C–H bond of CH_2 for the OH at **d** site (Figure S5) is activated by overcoming the larger energy barrier of 29.7 kcal/mol with endothermic by 21.7 kcal/mol, while the adsorbed OH at **e** site lowers the barrier to 17.1 kcal/mol, and the formation of intermediate is only less stable by 6.3 kcal/mol than the initial state (Figure S6). The spin densities (Figure S7) show that the H abstraction for GO2 with OH at **d** site leads to the larger magnetic moments located at GO, but for **e** site, it leads to the sublattice balance of graphene. Thus, the increased activity of epoxides by the neighboring OH group is attributed to the formation of nonmagnetic phase of GO. Owing to the small surface strain induced by the added OH, the initial structure of GO2-C_3H_8 is more favorable in energy than the GO2-2d-C_3H_8 and GO2-2e-C_3H_8.

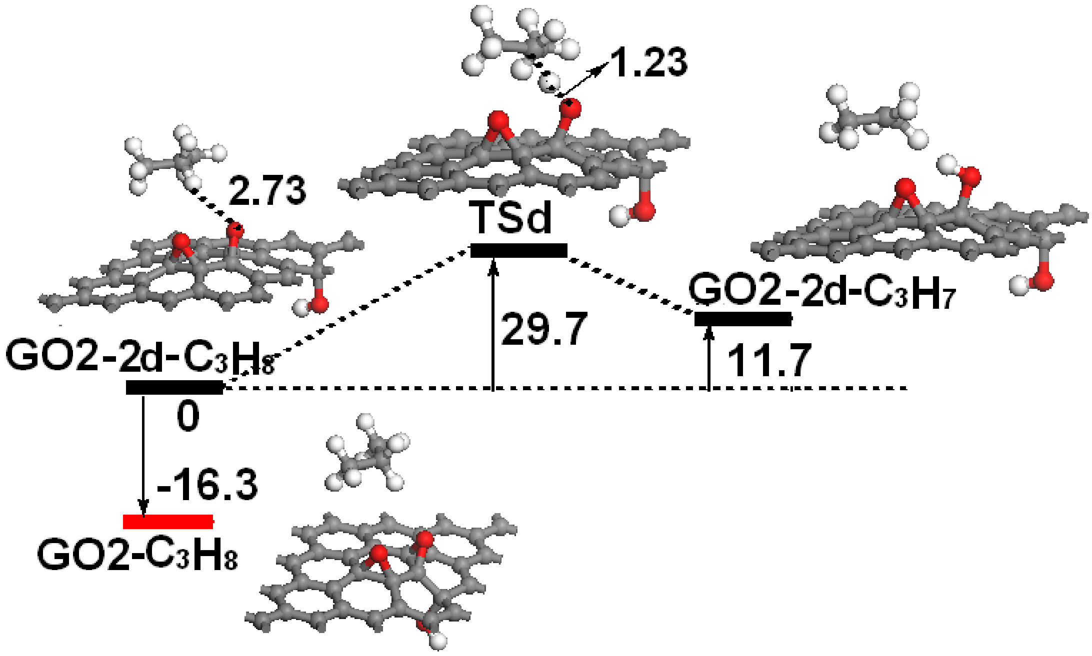

Figure S5. Energy profiles for the first H abstraction from CH_2 of propane on GO2-2d. All energies (in kcal/mol) are relative to propane adsorbed on GO2-2d, and the optimized configurations (distance in Å) of initial, transition, and final states are shown. For comparison, the initial structure of GO2-C_3H_8 is also shown.

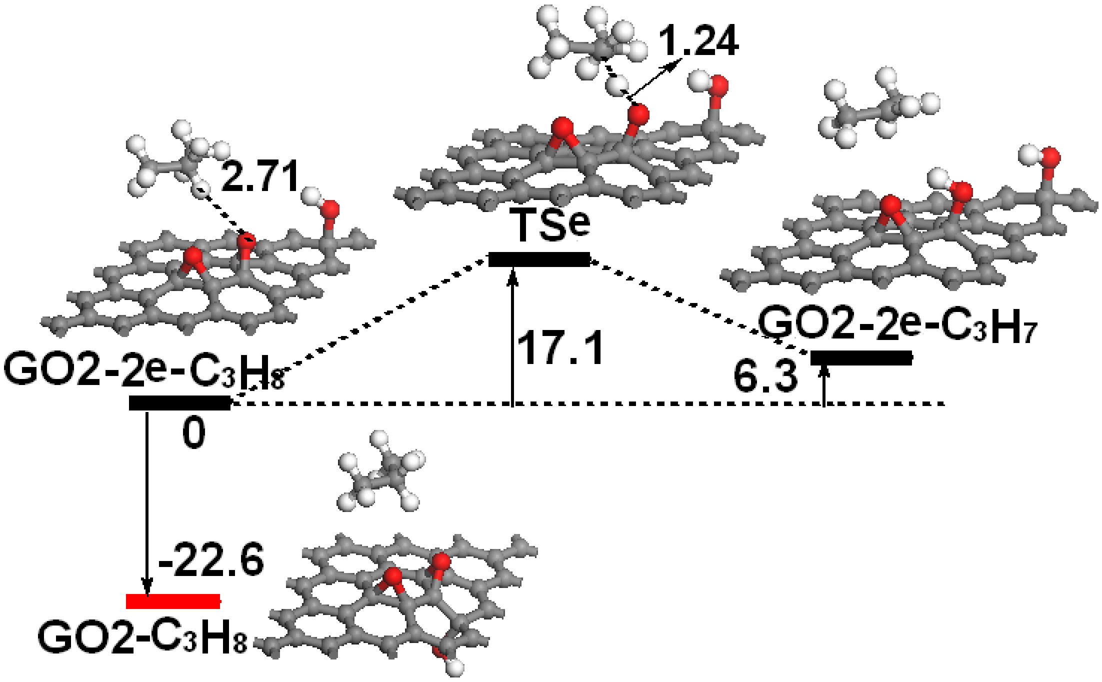

Figure S6. Energy profiles for the first H abstraction from CH_2 of propane on GO2-2e. All energies (in kcal/mol) are relative to propane adsorbed on GO2-2e, and the optimized configurations (distance in Å) of initial, transition, and final states are shown. For comparison, the initial structure of GO2-C_3H_8 is also shown.

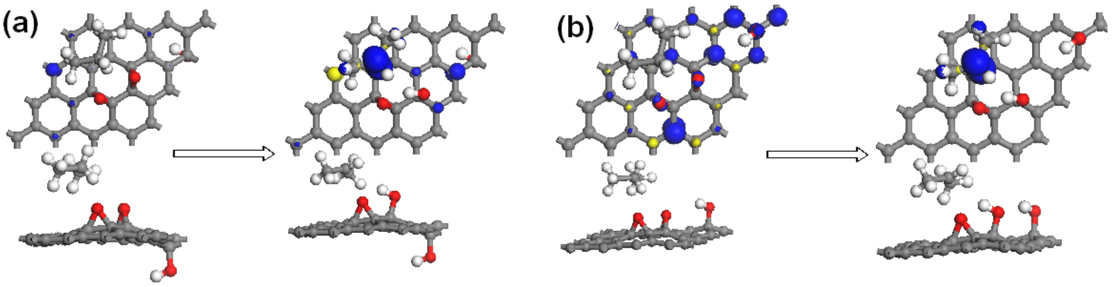

Figure S7. Optimized structures (top and side view) and spin densities (top view) for the conversion from propane to C_3H_7 on GO2 with one adsorbed OH at (a) **d** and (b) **e** sites. The isosurface is 0.03 *e*/Å^3 with blue for spin up and yellow for spin down.

4. Optimized structures and relative energy profiles for conversion from propane to C_3H_7 on GO2 with two OH groups at d and f sites.

For two OH groups at **f** and **d** sites of GO2, the barrier for C–H bond cleavage is predicted to be 32.1 kcal/mol, no activity enhancement is found compared to GO2 with only one OH at **d** site.

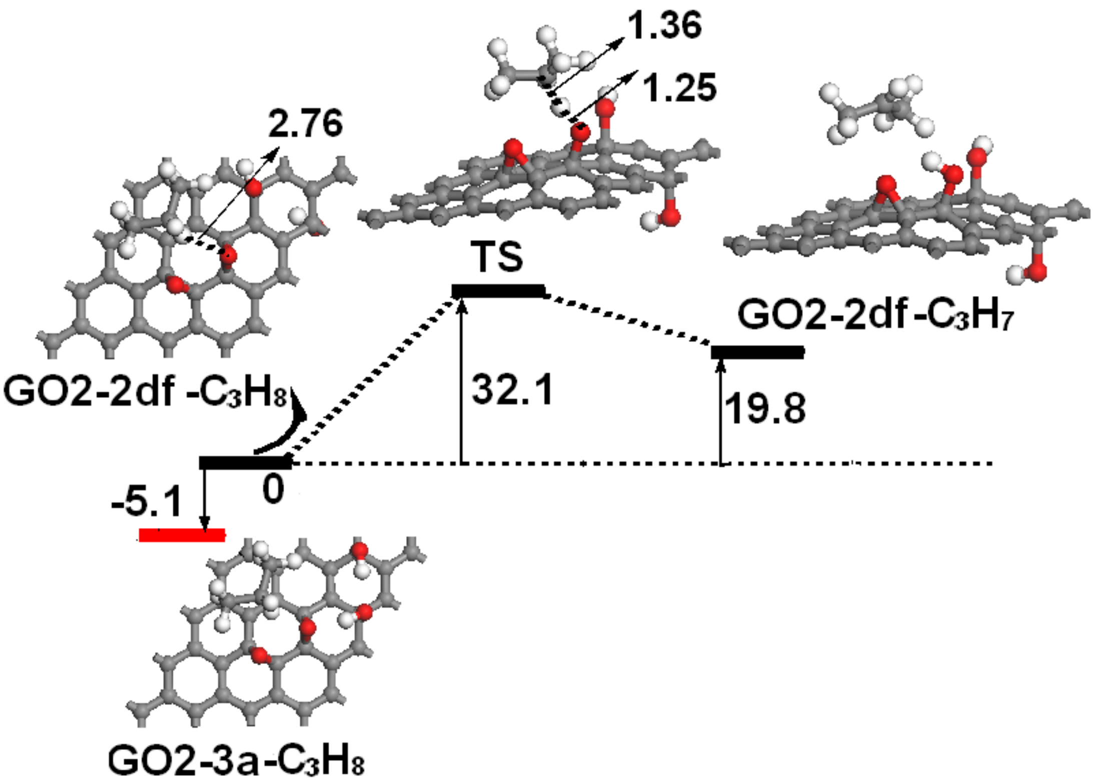

Figure S8. Energy profiles for the first H abstraction from CH_2 of propane on GO2 with two adsorbed OH groups at sites **d** and **f**. All energies (in kcal/mol) are relative to the initial structure, and the optimized configurations (distance in Å) of initial, transition, and final states are shown. For comparison, the initial structure of GO2-3a-C_3H_8 is also shown.